FORMATION OF η-MESIC NUCLEI*

Satoru Hirenzaki, Hideko Nagahiro

Department of Physics, Nara Women's University
Nara 630-8506, Japan

Daisuke Jido

Yukawa Institute for Theoretical Physics, Kyoto University
Kyoto 606-8502, Japan

In this paper, we briefly introduce the interests and the recent research activities on the η-mesic nuclei. We also mention the activities on the $\eta'(958)$-mesic nucleus formation.

1. Introduction

Meson-nucleus bound systems are considered to be very interesting objects in the contemporary hadron-nuclear physics. Especially, we can make use of them as *laboratories* for the studies of hadron properties at finite density which are closely related to the symmetry breaking and restoration patters of the strong interaction [1].

One of the most interesting results was obtained by observation of deeply bound pionic atoms [2]. Since the s-wave strength of the pion–nucleus optical potential is considered to provide the information on the pion decay constant f_π in nucleus, it is extremely interesting to study the s-wave part of the potential. For the purpose, it is highly required to observe the pionic s-states precisely because the s-states properties strongly depend on the s-wave potential [3] and, thus, the $1s$ states in heavy nuclei ($N > Z$) provide key information on the isovector part of the s-wave potential, which is related to f_π through the Tomozawa–Weinberg theorem [4]. According to this line, Suzuki *et al.* [5] performed an experiment based on the theoretical predictions [3,6], and obtained excellent new data of the deeply bound pionic

---

* Presented at International Symposium on Mesic Nuclei, Kraków, Poland, June 16, 2010.

$1s$ states in Sn isotopes, which helped much to deduce the new experimental information on the partial restoration of chiral symmetry in nucleus [5]. Thus, it is extremely interesting to extend this research field of meson bound systems to include other mesic systems.

In this paper, we report the recent research activities on the η-mesic nuclei. We also mention shortly the recent research activities on $\eta'(958)$-mesic nucleus.

2. η-nucleus systems

We discuss the η-nucleus systems in this report. We are interested in the η-mesic nuclei because they can be considered as a doorway to the study of the $N^*(1535)$ resonance (N^*) in nucleus due to the strong coupling of ηN and N^* [7]. The nature of the N^* is still controversial and there exist two different pictures of N^*, which provide significantly different η-nucleus potentials as shown below.

Around twenty years ago, the η-mesic nuclei were studied by Haider and Liu [8] and by Chiang, Oset and Liu [9]. As for the formation reaction, the attempt to find the bound states by the (π^+, p) reaction led to a negative result [10]. Recently, some experiments in photoproduction processes indicated observations of such bound states in ^{12}C target [11] and ^{3}He target [12]. A result of the proton induced reaction was reported in Ref. [13]. New experiments are also planed to investigate further the η-nucleus interaction and possible bound states [14, 15].

2.1. η-nucleus interaction based on $N^*(1535)$ dominance

Here, we briefly explain how the N^* nature affects the η-nucleus optical potential [16] using two theoretical models. In the η-nucleon system, the N^* resonance plays an important role due to the dominant $\eta N N^*$ coupling. Here we evaluate the η-nucleus optical potential $V_\eta(\omega, \rho(r))$ in the two different models which are based on distinct physical pictures of N^*. One is the chiral doublet model. This is an extension of the linear sigma model for the nucleon and its chiral partner [17–19]. We adopted a mirror assignment of the chiral doublet model in this paper. The other is the chiral unitary model, in which N^* is dynamically generated in the coupled channel meson–baryon scattering [20, 21]. We will compare the phenomenological consequences of these models based on the common assumption, the N^* dominance of the η-nucleon system.

In the first approach, the N^* is introduced as a particle with a large width and appears in an effective Lagrangian together with the nucleon field. Assuming N^*-hole excitation induced by the η meson in nucleus, we obtain the η-nucleus optical potential at finite nuclear density as

$$V_\eta(\omega, \rho(r)) = \frac{g_\eta^2}{2\mu} \frac{\rho(r)}{\omega + m_N^*(\rho) - m_{N*}^*(\rho) + i\Gamma_{N*}(\omega, \rho)/2}, \qquad (1)$$

in the local density approximation and the heavy baryon limit [9]. Here μ is the η-nucleus reduced mass and $\rho(r)$ is the density distribution of the nucleus. The ηNN^* coupling is assumed to be s-wave

$$\mathcal{L}_{\eta NN^*}(x) = g_\eta \bar{N}(x)\eta(x)N^*(x) + \text{H.c.}, \qquad (2)$$

and the coupling constant g_η is determined to be $g_\eta \simeq 2.0$ in order to reproduce the partial width $\Gamma_{N*\to\eta N} \simeq 75$ MeV at tree level. m_N^* and m_{N*}^* are the effective masses of N and N^* in the nuclear medium, respectively. Considering that the N^* mass in free space lies only 50 MeV above the threshold and that the mass difference of N and N^* might change in the medium, the η-nucleus optical potential is expected to be extremely sensitive to the in-medium properties of N and N^*. For instance, if the mass difference reduces in the nuclear medium as $m_\eta + m_N^* - m_{N*}^* > 0$, then the optical potential turns to be repulsive [16].

In the chiral doublet model together with the expected partial restoration of chiral symmetry, a reduction of the mass difference of N and N^* in the medium is found to be in the mean field approximation as [17,18,22,23]

$$m_N^*(\rho) - m_{N*}^*(\rho) = \Phi(\rho)(m_N - m_{N*}), \qquad (3)$$

where m_N and m_{N*} are the N and N^* masses in free space, respectively, and

$$\Phi(\rho) = 1 - C\frac{\rho}{\rho_0}. \qquad (4)$$

Here we take the linear density approximation of the in-medium modification of the chiral condensate, and the parameter C represents the strength of the chiral restoration at the nuclear saturation density ρ_0. The empirical value of C lies from 0.1 to 0.3 [24]. Here we perform our calculations with $C = 0.0$ and 0.2 in order to clarify the effects of the partial restoration of chiral symmetry.

In Fig. 1, we show the η-nucleus optical potentials obtained by the chiral doublet model with $C = 0.0$ and $C = 0.2$ in the case of the η–^{11}B system [16]. As shown in the figure, the η-nucleus optical potential has a curious shape of a repulsive core inside nucleus and an attractive pocket in nuclear surface. The qualitative feature of the optical potential discussed here, such as the appearance of the repulsive core in the case of $C = 0.2$, is independent of type of nuclei. Thus, it is extremely interesting to confirm the existence (or non-existence) of this curious shaped potential experimentally.
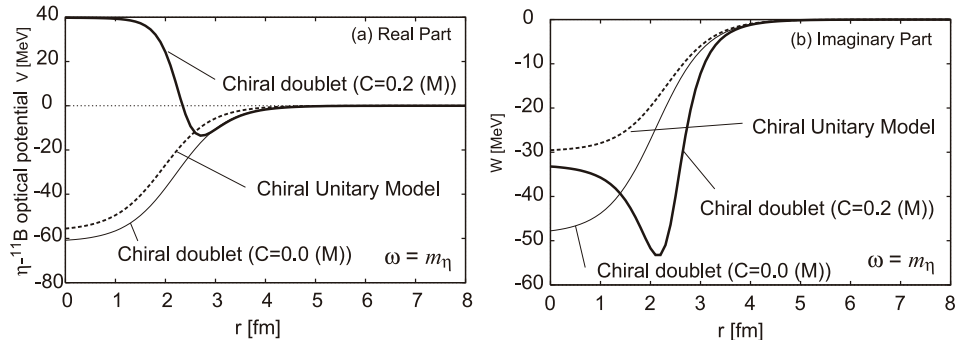
Fig. 1. The η-nucleus optical potential for the η–^{11}B system as functions of the radius coordinate r reported in Ref. [16]. The left and right figures show the real part and the imaginary part of the η-nucleus optical potential, respectively. In both figures, the solid lines show the potentials of the chiral doublet model with $C = 0.2$ (thick line) and $C = 0.0$ (thin line), and dashed lines show that of the chiral unitary model, which is picked from the results shown in Ref. [20].

Let us move on the second approach of the chiral unitary model [20, 21]. In this approach, the N^* resonance is expressed as a dynamically generated object in the meson–baryon scattering, and one solves a coupled channel Bethe–Salpeter equation to obtain the η-nucleon scattering amplitude. The optical potential in medium is obtained by closing the nucleon external lines in the ηN scattering amplitude and considering the in-medium effect on the scattering amplitude, such as Pauli blocking. Since the N^* in the chiral unitary approach is found to have a large component of $K\Sigma$ and the Σ hyperon is free from the Pauli blocking in nuclear medium, very little mass shift of N^* is expected in the medium [25], while the chiral doublet model predicts the significant mass reduction with the partial restoration of chiral symmetry as discussed above. The optical potential obtained by the chiral unitary approach in Ref. [20] is also shown in Fig. 1, and the potential resembles that of the chiral doublet model with $C = 0.0$ due to the small medium effect.

The calculated binding energies and widths for both potentials are reported in Refs. [16, 20]. As we can expect from the potential shapes, they show the significant differences, which are expected to be observed in the spectra of the formation reactions of η-nucleus systems.

2.2. Green's function method

We use the Green's function method [26] to calculate the formation spectra of the meson-nucleus systems [16, 27–36]. We briefly explain the formalism for the (π, N) reaction case as an example. The expected spectra of the

(π, N) reactions $\left(\frac{d^2\sigma}{d\Omega dE_N}\right)$ are evaluated from the nuclear response function $S(E)$ and the elementary cross-section $\left(\frac{d\sigma}{d\Omega}\right)^{\mathrm{ele}}$ in the impulse approximation as

$$\left(\frac{d^2\sigma}{d\Omega dE_N}\right) = \left(\frac{d\sigma}{d\Omega}\right)^{\mathrm{ele}} \times S(E). \tag{5}$$

The calculation of the nuclear response function with a meson-nucleus complex optical potential V_{opt} is formulated by Morimatsu and Yazaki [26] as

$$S(E) = -\frac{1}{\pi}\mathrm{Im}\sum_f \int d\vec{r}d\vec{r}' \tau_f^\dagger G(E;\vec{r},\vec{r}')\tau_f, \tag{6}$$

where the summation is taken over all possible final states. $G(E;\vec{r},\vec{r}')$ is the Green's function of the produced meson interacting in the nucleus and defined as

$$G\left(E;\vec{r},\vec{r}'\right) = \langle\alpha|\phi(\vec{r})\frac{1}{E - H + i\epsilon}\phi^+(\vec{r}')|\alpha\rangle, \tag{7}$$

where α indicates the proton hole state and H indicates the Hamiltonian of the meson-nucleus system, which includes the optical potential V_{opt}. The amplitude τ_f denotes the transition of the incident particle (π) to the nucleon–hole and the outgoing nucleon (N), involving the nucleon–hole wavefunction ψ_{j_N} and the distorted waves χ_i and χ_f of the projectile and ejectile. By taking the appropriate spin sum, the amplitude τ_f can be written as

$$\tau_f(\vec{r}) = \chi_f^*(\vec{r})\xi_{1/2,m_s}^*\left[Y_l^*\left(\hat{\vec{r}}\right) \otimes \psi_{j_N}(\vec{r})\right]_{JM}\chi_i(\vec{r}), \tag{8}$$

with the meson angular wavefunction $Y_l(\hat{\vec{r}})$ and the spin wavefunction $\xi_{1/2,m_s}$ of the ejectile.

The semi-exclusive spectra can be calculated by decomposing the response function (6) into the escape and conversion parts: $S = S_{\mathrm{esc}} + S_{\mathrm{con}}$. The conversion part and the escape part are known to express the contributions to the (π, N) spectra of the meson absorption in nucleus and the quasi-elastic meson production processes, respectively [26].

2.3. Formation by (π, N) reactions

We show in Fig. 2 the calculated $^{12}\mathrm{C}(\pi^+, p)^{11}\mathrm{C}\otimes\eta$ cross-sections for the formation of the η-$^{11}\mathrm{C}$ system with the chiral doublet model potential for $C = 0.2$ (left panel) and that of the chiral unitary model (right panel) [35]. The incident pion kinetic energy T_π is 820 MeV corresponding to the recoilless condition at the η threshold. The horizontal axis indicates the excitation energy E_{ex} defined as

$$E_{\text{ex}} = m_\eta - B_\eta + (S_n(j_n) - S_n(\text{ground})), \qquad (9)$$

where B_η is the η binding energy and $S_n(j_n)$ the neutron separation energy from the neutron single-particle level j_n. $S_n(\text{ground})$ indicates the separation energy from the neutron level corresponding to the ground state of the daughter nucleus and $E_0 = m_\eta$. Hence $E_{\text{ex}} - E_0 = 0$ corresponds to the η production threshold with the ground state daughter nucleus.
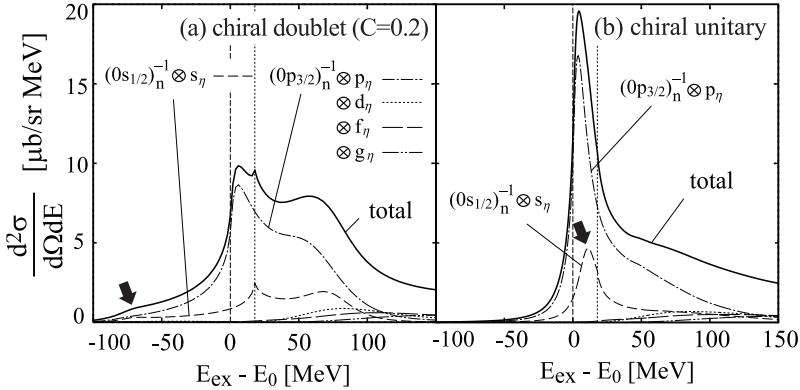

Fig. 2. Calculated spectra of the $^{12}\text{C}(\pi^+, p)^{11}\text{C}\otimes\eta$ reaction at $T_\pi = 820$ MeV and the emitted proton angle $\theta_p = 0°$ as functions of the excited energy E_{ex} [35]. E_0 is the η production threshold. The η-nucleus interaction is calculated by using (a) the chiral doublet model with $C = 0.2$ and (b) the chiral unitary model. The thick solid lines show the total spectra and the dashed lines represent dominant subcomponents as indicated in the figures. The neutron–hole states are indicated as $(n\ell_j)_n^{-1}$ and the η states as ℓ_η. The solid arrow indicates the peak due to the bound state in each model.

In the figure, we show the total spectra by the solid line and the contributions from dominant subcomponents by the dashed lines, separately. We take into account the difference of the separation energy $S_n(j_n) - S_n(\text{ground})$ = 18 MeV for a subcomponent accompanied by a $(0s_{1/2})_n^{-1}$ hole-state. In such a case, the η-meson production threshold appears at $E_{\text{ex}} - E_0 = 18$ MeV as indicated in Fig. 2 by the vertical dotted line. The Fig. 2 shows that the spectra are dominated by two contributions, $(0s_{1/2})_n^{-1} \otimes s_\eta$ and $(0p_{3/2})_n^{-1} \otimes p_\eta$, since the final states with the total spin $J \sim 0$ are largely enhanced under the recoil-free kinematics.

Let us see the spectra around the threshold; -50 MeV $\lesssim E_{\text{ex}} - E_0 \lesssim$ 50 MeV. The spectra in this energy region were already shown in the case of the $(d, {}^3\text{He})$ and (γ, p) reactions in Refs. [16, 33]. The present work confirms that the spectral shape is very similar with the previous calculations showing

that the structure of the formation spectra is not sensitive to the reaction mechanism. As already discussed in detail in Refs. [16, 33], the spectra with the (π^+, p) reaction around the η production threshold show that the repulsive nature of the optical potential in the chiral doublet model shifts the spectra into the higher energy region, whereas the spectra obtained in the chiral unitary model is shifted into the lower energy region as a result of its attractive potential.

We conclude that the difference between the expected spectra with two chiral models seems to be visible in the (π^+, p) reaction as well as the (γ, p) reaction in spite of the distortion effect for the injected particle π. The systematic results and the detail discussions are found in Ref. [35].

2.4. Formation by $d + d$ reactions — preliminary results

The η-nucleus optical potential has large imaginary part in general, which makes the decay widths of the possible bound states large and makes the observation of distinct peak structures in the spectrum difficult. Thus, it is interesting to consider the systems of η in light nuclei because we can expect to avoid the additional difficulties due to overlaps of many subcomponents to deduce the physical information from the observed spectrum.

In this subsection, we consider the formation reaction of the $\eta + \alpha$ system proposed in Ref. [14]. We have evaluated the formation rate of the $\eta + \alpha$ system using the Green's function method. We have paid the special attention to calculate both cross-sections of the η production $d + d \to \alpha + \eta$ reaction and the bound state formation $d + d \to (\alpha\eta)_{\text{bound}}$ using the same model simultaneously. This is important to reduce the uncertainties of the theoretical calculation due to the nuclear transition form factor in the very high momentum transfer reaction (~ 1 GeV/c) by using the $d + d \to \alpha + \eta$ data near threshold [37]. We have developed a simple theoretical model for the reaction, where we include one parameter to control the nuclear transition form factor $(d + d \to \alpha)$ with η production in addition to the η-nucleus optical potential strength. The details of the theoretical model will be described in Ref. [38].

We show the preliminary results in Fig. 3 where we have assumed the depth of the η-nucleus optical potential as $V_\eta(0) = (-50 - 40i)$ MeV at nuclear center, which are similar with those of chiral unitary model. The absolute value of the cross-section is scaled to fit the data [37]. We found that the shape of the $d + d \to \alpha + \eta$ data were reproduced reasonably well by the escape part of the spectrum. The conversion part corresponding to the contribution of the η absorption process by nucleus is found to have peak structure at the threshold on the large structureless background. The results of this model will provide useful estimates for the planned experiment [14] where the particle pair emissions from η absorption will be measured.
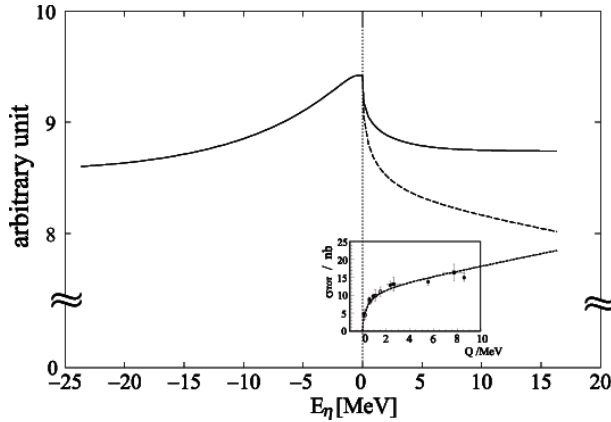
Fig. 3. Calculated spectra of the $d + d \rightarrow \alpha + \eta$ reaction are plotted as functions of the kinetic energy of η. The negative energy region corresponds to the formation of (subthreshold) $\eta + \alpha$ bound system. The η production threshold is shown as a vertical dotted line. Solid and dashed curves show the total spectrum and conversion part, respectively. The escape part is also shown as a dotted curve and compared with experimental data above threshold [37].

The calculated spectrum shape is found to be sensitive to the optical potential strengths and to the (non-)existence of the bound states. Thus, we think the experimental data will provide new information on the η-nucleus interaction. The systematic numerical results will be reported in Ref. [38].

2.5. $\eta'(958)$-nucleus systems

As for the formation of other meson-nucleus systems, we mention here another research activity. The $\eta'(958)$-nucleus systems are very interesting because the origin of its large mass is believed to be the consequences of the $U_A(1)$ anomaly effects. Structure and formation reaction of the $\eta'(958)$-nucleus systems were studied in Ref. [31] for the first time, and the formation of this system by (π, N) reactions are also reported in Ref. [39], recently. We can expect to have important information on the anomaly effects at finite density, which has not been known at all so far, by studying the $\eta'(958)$-nucleus systems.

3. Conclusion

The mesic atoms and mesic nuclei are very interesting and fruitful objects to study the aspects of the strong interaction symmetries at finite density. We briefly explain the recent research activities on η-mesic nuclei.

We think that the theoretical results reported here will help to consider future experiments and to obtain new information on meson and/or baryon resonance such as N^* properties in nucleus from data.

S.H. thanks P. Moskal for the invitation to this stimulating meeting and the hospitality during the stay in Kraków.

REFERENCES

[1] T. Hatsuda, T. Kunihiro, *Phys. Rep.* **247**, 221 (1994) and references therein.

[2] H. Toki, T. Yamazaki, *Phys. Lett.* **B213**, 129 (1988); H. Toki, S. Hirenzaki, T. Yamazaki, R.S. Hayano, *Nucl. Phys.* **A501**, 653 (1989).

[3] Y. Umemoto, S. Hirenzaki, K. Kume, H. Toki, *Phys. Rev.* **C62**, 024606 (2000).

[4] E.E. Kolomeitsev, N. Kaiser, W. Weise, *Phys. Rev. Lett.* **90**, 092501 (2003); D. Jido, T. Hatsuda, T. Kunihiro, *Phys. Lett.* **B670**, 109 (2008).

[5] K. Suzuki *et al.*, *Phys. Rev. Lett.* **92**, 072302 (2004).

[6] S. Hirenzaki, H. Toki, T. Yamazaki, *Phys. Rev.* **C44**, 2472 (1991).

[7] C. Amsler *et al.* [Particle Data Group], *Phys. Lett.* **B667**, 1 (2008).

[8] Q. Haider, L.C. Liu, *Phys. Lett.* **B172**, 257 (1986); *Phys. Rev.* **C34**, 1845 (1986).

[9] H.C. Chiang, E. Oset, L.C. Liu, *Phys. Rev.* **C44**, 738 (1991).

[10] R.E. Chrien *et al.*, *Phys. Rev. Lett.* **60**, 2595 (1988).

[11] G.A. Sokol *et al.*, *Fizika* **B8**, 85 (1999).

[12] M. Pfeiffer *et al.*, *Phys. Rev. Lett.* **92**, 252001 (2004).

[13] A. Budzanowski *et al.*, *Phys. Rev.* **C79**, 012201 (2009).

[14] P. Moskal, `arXiv:nucl-ex/09093979`; P. Moskal *et al.*, Proposal at COSY, 186.2.

[15] K. Itahashi *et al.*, LOI for JPARC 2007.

[16] D. Jido, H. Nagahiro, S. Hirenzaki, *Phys. Rev.* **C66**, 045202 (2002); H. Nagahiro, D. Jido, S. Hirenzaki, *Phys. Rev.* **C68**, 035205 (2003).

[17] C. DeTar, T. Kunihiro, *Phys. Rev.* **D39**, 2805 (1989).

[18] D. Jido, M. Oka, A. Hosaka, *Prog. Theor. Phys.* **106**, 873 (2001); D. Jido, Y. Nemoto, M. Oka, A. Hosaka, *Nucl. Phys.* **A671**, 471 (2000).

[19] Y. Nemoto, D. Jido, M. Oka, A. Hosaka, *Phys. Rev.* **D57**, 4124 (1998).

[20] C. Garcia-Recio, J. Nieves, T. Inoue, E. Oset, *Phys. Lett.* **B550**, 47 (2002); T. Inoue, E. Oset, *Nucl. Phys.* **A710**, 354 (2002).

[21] N. Kaiser, T. Waas, W. Weise, *Nucl. Phys.* **A612**, 297 (1997).

[22] T. Hatsuda, M. Prakash, *Phys. Lett.* **B224**, 11 (1989).

[23] H. Kim, D. Jido, M. Oka, *Nucl. Phys.* **A640**, 77 (1998).

[24] T. Hatsuda, T. Kunihiro, H. Shimizu, *Phys. Rev. Lett.* **82**, 2840 (1999).

[25] N. Kaiser, P.B. Siegel, W. Weise, *Phys. Lett.* **B362**, 23 (1995).

[26] O. Morimatsu, K. Yazaki, *Nucl. Phys.* **A435**, 727 (1985); **A483**, 493 (1988).

[27] K. Ikuta, M. Arima, K. Masutani, *Prog. Theor. Phys.* **108**, 917 (2002).

[28] J. Yamagata, H. Nagahiro, S. Hirenzaki, *Phys. Rev.* **C74**, 014604 (2006).

[29] T. Koike, T. Harada, *Phys. Lett.* **B652**, 262 (2007); *Nucl. Phys.* **A804**, 231 (2008).

[30] J. Yamagata-Sekihara, D. Jido, H. Nagahiro, S. Hirenzaki, *Phys. Rev.* **C80**, 045204 (2009).

[31] H. Nagahiro, S. Hirenzaki, *Phys. Rev. Lett.* **94**, 232503 (2005); H. Nagahiro, M. Takizawa, S. Hirenzaki, *Phys. Rev.* **C74**, 045203 (2006).

[32] R.S. Hayano, S. Hirenzaki, A. Gillitzer, *Eur. Phys. J.* **A6**, 99 (1999).

[33] H. Nagahiro, D. Jido, S. Hirenzaki, *Nucl. Phys.* **A761**, 92 (2005).

[34] D. Jido, E.E. Kolomeitsev, H. Nagahiro, S. Hirenzaki, *Nucl. Phys.* **A811**, 158 (2008).

[35] H. Nagahiro, D. Jido, S. Hirenzaki, *Phys. Rev.* **C80**, 025205 (2009).

[36] J. Yamagata-Sekihara, D. Cabrera, M.J. Vicente Vacas, S. Hirenzaki, *Prog. Theor. Phys.* (2010), in print.

[37] R. Frascaria *et al.*, *Phys. Rev.* **C50**, 537 (1994); N. Wills *et al.*, *Phys. Lett.* **B406**, 14 (1997); A. Wronska *et al.*, *Acta. Phys. Pol. A* **56**, 279 (2006).

[38] S. Hirenzaki, H. Nagahiro, D. Jido, in preparation.

[39] H. Nagahiro, Proceedinds of the YITP international workshop "New Frontiers in QCD 2010" (NFQCD10), *Prog. Theor. Phys. Suppl.*, submitted.